RSC Advances

ROYAL SOCIETY OF CHEMISTRY

www.rsc.org/advances

Graphical Abstract

A luminescent $[Tb_2(BDC)_3(H_2O)_4]_n$ film with a leaf-like morphology is fabricated on FTO by electrochemical method, the film exhibits highly selective detection of Cu^{2+}.

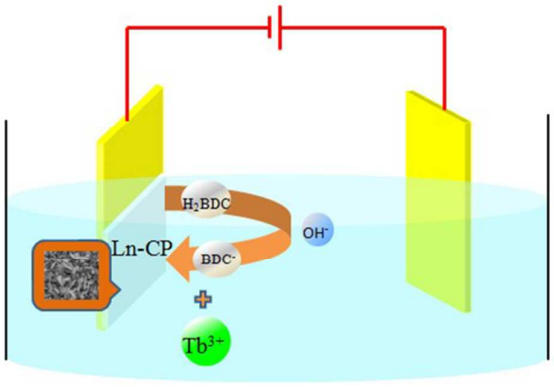

Cite this: DOI: 10.1039/c0xx00000x

www.rsc.org/xxxxxx

ARTICLE TYPE

One step cathodically electrodeposited $[Tb_2(BDC)_3(H_2O)_4]_n$ thin film as a luminescent probe for Cu^{2+} detecting

Yi Wang [a], Tianshu Chu[a], Minghao Yu [a], Huiping Liu [a]and Yangyi Yang*[a]

Received (in XXX, XXX) Xth XXXXXXXXX 20XX, Accepted Xth XXXXXXXXX 20XX

DOI: 10.1039/b000000x

A luminescent Ln-CPs film of $[Tb_2(BDC)_3(H_2O)_4]_n$ (**1**) [BDC: *p*-benzenedicarboxylate anion] is fabricated using electrodeposited method on FTO (fluorine-doped tin oxide glass). It is a one-step and highly effective electrochemical method at room temperature. The influence of reaction conditions on thickness of film **1** was investigated. The smooth and adherent thin film **1** is obtained at the proper concentrations of $Tb(NO_3)_3$ (0.01 M) and H_2BDC (0.015 M) with 0.3 mA/cm^2 (0.050 M NH_4NO_3) for 20 minutes. The composition of the film was confirmed by X-ray diffraction. The sensing properties of the film have been studied. The result shows that thin film **1**exhibits selective detection of Cu^{2+} in DMF solution. The luminescent intensity is inversely proportional to the concentration of Cu^{2+} ions and displays a linear region over the range of 1×10^{-5} -1×10^{-3} M. Furthermore, a probable quenching mechanism was discussed.

1 Introduction

In recent years, the design and syntheses of lanthanide coordination polymers (Ln-CPs) are attracting increasing attention for a wide variety of applications in the fields of magnetism, catalyst,[1] gas storage and separation.[2] Ln-CPs shows excellent luminescent properties, such as long lifetime, high color purity and intense sharp emission in near-infrared and visible region ranges.[3-5] It should be noted that the unique luminescence properties of Ln-CPs result from f −f transitions generated by the "antenna effect", which have made them one of the essential components in the preparation of advanced materials. Recently, studies on luminescent Ln-CPs for sensing metal ions have resulted in their significant development, and some successful fluorescent probes have been employed to determine the concentration of metal ions[6, 7] and anions[8, 9] in solution. These applications are usually based on CPs in the powder form. For practical sensor applications, it is very necessary to develop Ln-CPs films for the straightforward sensing of metal ions or vapor.[10-16] Ln-CPs are commonly processed into thin film by several methods, such as high-vacuum thermal evaporation,[17] layer-by-layer deposition[18] and galvanic displacement.[10] The main drawback of these methods remains the large amounts of waste that are produced during the synthesis, especially expensive metal salts.

In order to avoid such drawbacks, an electrochemical synthesis method which is becoming more attractive for the deposition of new materials[19, 20] was proposed. Electrochemical one-step deposition is an interesting alternative route for the preparation of such materials, especially if deposition on conductive substrates is desirable. Compared to above methods, one-step electrodeposition is rather easy to carry out. High temperatures or vacuum conditions are not needed, which makes the process economically interesting and allows the use of flexible conductive plastic substrates that are not stable at higher temperatures.[21, 22] In recent years, although some work has been focused on developing CPs by electrochemical synthesis method,[13, 23-26] to our knowledge, there have been a few reports on the respective CPs film produced electrochemically.

Cu^{2+} obviously plays a role in the areas of many fundamental biological and environmental system.[27] It is an essential trace element for both plants and animals, including humans. However, Several research studies have linked the cellular toxicity of copper ions to serious diseases such as Alzheimer's disease,[28] prion diseases.[29] Many analytical methods have been performed for detection of Cu^{2+}, such as atomic absorption spectrometry (AAS),[30] inductively coupled plasma-emission spectrometry (ICP-ES).[31] These methods usually have a sufficiently low detection limit and have disadvantages such as more complicated and high cost apparatus, and time-consuming procedures.[32] Recently, more attention has been focused on the development of luminescent chemosensors for the detection of Cu^{2+} ions.

In our previous work, many Ln-CPs have been synthesized. Most of them exhibit extraordinary luminescent properties.[8, 33-36]

The rational design and preparation of desired Ln-CPs remain a great challenge because of the high coordination numbers and variable nature of the Ln^{3+} sphere. It has proven to be an effective method for the design and synthesis of open and rigid frameworks through the assembly of Ln-carboxylate clusters with organic linkers. *p*-benzenedicarboxylic acid (H_2BDC) seems to be a promising organic linker due to its rigid structure, diversity of coordination geometries, various coordination modes. A large number of CPs made up of metals and H_2BDC have been reported, and many of them show excellent adsorption and gas-

storage properties. Compared with transition metals, the analogous lanthanide coordination polymers are still undeveloped.[37] Encouraged by aforementioned studies, the luminescent film of $[Tb_2(BDC)_3(H_2O)_4]_n$ (**1**) is fabricated by one-step convenient electrodeposited method in this paper. The influence of reaction conditions on thickness of film **1** is investigated. The smooth and adherent thin film **1** is obtained under the optimized condition. The luminescence responses of thin film **1** toward various metal ions in DMF solution exhibits highly selective detection of Cu^{2+}. The possible sensing mechanism based on static quenching is discussed. Moreover, this result may provide useful information to further develop more Ln-CPs films with applications in luminescent sensors.

2 Experimental sections

2.1 Materials and Instrumentation

All reagents were purchased from commercial sources and used directly without further purification. DMF solutions of Co^{2+}, Ni^{2+}, Cu^{2+}, Zn^{2+}, Cd^{2+}, K^+, Na^+ and Pb^{2+} were prepared from their nitrate salts; deionized water was used throughout all experiments. All steady state luminescence measurements were recorded by Himadzu RF-5301 PC spectrofluorophotometer at room temperature in the range of 450–650 nm with a fixed excitation wavelength of 323 nm. Luminescence lifetimes were collected by FLSP920 fluorescence spectrometer. X-ray diffraction (XRD) measurements were performed on a D/MAX 2200VPC diffractometer with Cu Kα radiation (λ = 1.5406 Å) at a voltage of 30 kV and a current of 30 mA/cm^2. Crystalline peaks observed on the FTO substrate correspond to tin oxide (SnO_2, JCPDS file No. 01-075-9494, CSD#157449). Calculated PXRD patterns were produced by using the software of Mercury, Jade 6.5 and origin 8.0. The size and surface morphologies of film **1** were observed by a scanning electron microscope (SEM, S-4800, Hitachi). Electrochemistry experiments were carried out on Potentiostat DJS-292B (shanghai China) and Metrohm PGSTAT 302N electrochemical workstation.

2.2 Preparation of thin film

Before the experiment, FTO (fluorine-doped tin oxide glass) conductive glass was cut into small pieces (about 25×10 mm^2). FTO and graphite rod (4 cm) were cleaned with acetone and methanol in ultrasonic bath 15 minutes respectively.

Firstly, 0.2 mmol $Tb(NO_3)_3{\cdot}6H_2O$ and 0.3 mmol H_2BDC were dissolved in 20 mL DMF solution and stirred until a clear solution was obtained. NH_4NO_3 (supporting electrolyte) was added to the solution with subsequent stirring 20 minutes at room temperature.

Film **1** was deposited onto FTO by galvanostat method. The working electrode was FTO (cathode) and the counter electrode (anode) was graphite rod. The two electrodes were separated by 5 cm and were partially immersed in the solution.

When the process was done, the deposited film was removed from the DMF solution and cleaned with DMF three times to remove unreacted ligands and Tb^{3+} ions.

2.3 Procedure for detection of Cu^{2+} ions

Stock standard solutions 0.01 M Cu^{2+} were prepared by dissolving 22.3 mg $Cu(NO_3)_2{\cdot}2H_2O$ in DMF and adjusting the volume to 10 mL in a volumetric flask. It was further diluted to 1×10^{-3} to 1×10^{-5} M stepwise. Similar procedure was performed for other metal ions. The luminescent intensity of thin film **1** (immersed in DMF solution) was recorded from 450 to 650 nm with excitation wavelength fixed at 323 nm. After thin film **1** was immersed in 1×10^{-3} M Cu^{2+} DMF solution for 36 hours, the luminescent intensity was again recorded. Similar procedure was performed for various predetermined concentrations of Cu^{2+} ions and other metal ions. All measurements were made at room temperature.

2.4 Principles of luminescent quenching

Fluorescence quenching commonly originated from dynamic quenching. And dynamic quenching can be described by the Stern-Volmer equation.[38] F_0 and F are the luminescent intensities before and after the addition of the quencher, respectively. k_q is the rate constant of dynamic quenching; τ_0 and τ is the lifetime in the absence or presence of the quenchers; [M] is molar concentration of the quencher in solution.

$$F_0/F = \tau_0/\tau = 1+k_q\tau_0[\mathrm{M}] \quad (1)$$

Another type of quenching (static quenching) occurs as a result of the formation of a non-luminescent complex between the fluorophore and quencher. For this type of quenching, the decrease of luminescent intensity has the same form as the Stern-Volmer Eq (1). However, in Eq (2) the K_{SV} is now the association constant.[38] Since the life-time of the luminescence is unperturbed by the static quenching τ_0/τ=1, lifetime measurements are a definitive method to distinguish between static and dynamic quenching.

$$F_0/F = 1+K_{SV}[\mathrm{M}] \quad (2)$$

3 Results and discussion

3.1 Influence of electrochemical parameters

Smooth, adherent films **1** were deposited from the $Tb(NO_3)_3{\cdot}6H_2O$, H_2BDC and NH_4NO_3 DMF solution over a range of current densities, deposition time and concentration of support electrolyte of the deposition bath.

The films electrodeposited at different current densities containing 0.1, 0.3 and 0.6 mA/cm^2 (t = 20 min, $c(NH_4NO_3)$ = 0.05 M) were discussed. When current density was 0.1 mA/·cm^2, smooth and adherent film was not obtained. When current density increased to 0.3 mA/cm^2, smooth and adherent thin film was obtained. While at higher current densities, the floccules can be observed near the cathode in the solution. This may be explained in the following way: at low current, the reaction rate was slow; the film under these conditions should be smooth and adherent. However, when current density exceeded a critical value (0.6 mA/cm^2), floccules developed near the electrode in solution. This can be attributed to the high over potential, which speed up the reaction rate. As a result, the formation of CPs took place near the cathode in solution rather than on the electrode.

Deposition time was one of the main factors affecting the thickness (J = 0.3 mA/cm^2 $c(NH_4NO_3)$ = 0.05 M). If the deposition time was not sufficient, the adherent and smooth film

was not obtained. The effect of deposition time on the thickness in the range of 10-30 min was studied. As the deposition time increased from 10 to 20 min, the thickness increased. And with further prolonging of the deposition time the thickness of film did not significantly increase (see Fig. S1).

The films electrodeposited in reaction solution containing different concentration of NH_4NO_3 (0.025, 0.050, 0.100 M) was discussed when current density and time (J = 0.3 mA/cm^2, t = 20 min) were fixed. By increasing the concentration of NH_4NO_3, conductivity increases. The conductivity increased with the increasing of concentration of NH_4NO_3. It was expected that higher conductivity would result in higher thickness of film.[39] However, it was worth noting that an increase in the concentration of support electrolyte did not translate into a proportional increase in thickness of film deposited in 0.050 and 0.100 M (see Fig S2). This phenomenon may be explained as followed: in this concentration range, the concentration of support electrolyte has slight effect on the thickness of film.

Taking the factors into account, the adherent and smooth film was obtained under the optimized conditions of J = 0.3 mA/cm^2, t= 20 min and $c(NH_4NO_3)$ = 0.05 M.

3.2 Characterization of thin film 1

Fig. 1 shows the morphological structure (SEM image) of the electrodeposited thin film **1**. Morphological studies clearly shows the 2 μm crystals merge tightly with each other leading into a continuous film.

According to the experimental results, it is easy to infer that deposition of such thin film **1** only in a few minutes proves a much faster growth rate than available with most other CPs surface deposition methods.

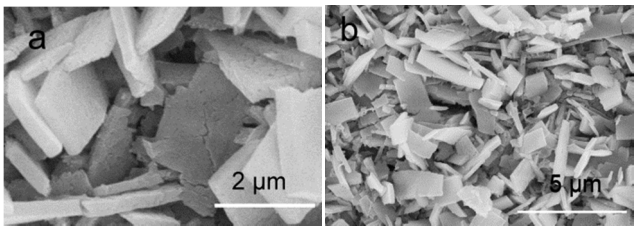

Fig. 1 The (a) enlarged top view SEM images of film **1** and (b) greater range top view

In order to study the formation process of thin film **1**, chronopotentiometry is studied. As shown in Fig. 2, after an initial voltage drop from the open circuit potential to -0.65 V (Ref. SCE), the electrode potential increases almost linearly during the first 3 minutes and subsequent slight increase. The increasing voltage that sustains the process is presumably related to the thickening of the deposits. This behaviour can be explained by the film growth, which takes place by initial nuclei formation and subsequent growth of these seed crystals.

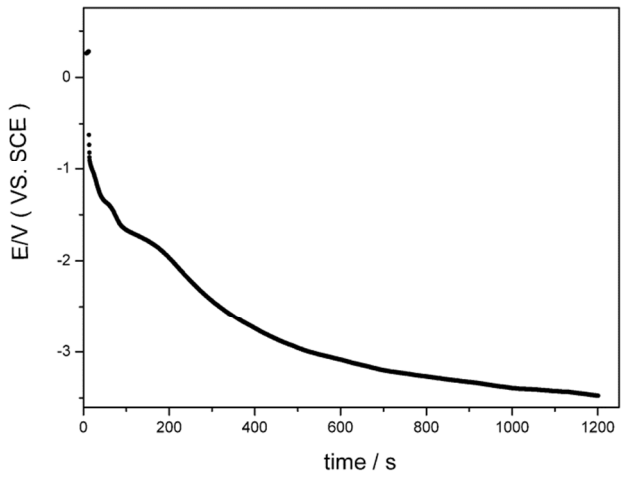

Fig. 2 Potential (Ref. SCE) vs. time curve during the electrodeposition of film **1**. Experimental conditions: J = 0.3 mA/cm^2 t = 20 min $c(NH_4NO_3)$ =0.05 M.

Fig. 3 shows the powder X-ray diffraction patterns of film **1**. All the diffraction maxima in the pattern of the as-deposited film **1** is consistent with the simulated data.[40] The overall structure of $[Tb_2(BDC)_3(H_2O)_4]_n$ can be described in terms of a parallelepipedal motif having a terbium center on each of its eight corners and BDC on four of its faces. Each Tb atom is coordinated in a monodentate fashion to six oxygens of BDC anions and two water ligands to give an eight-coordinate Tb(III) center. It should be noted that the water ligands occupy the other two faces of parallelepipedal motif, which allows them to point nearly to the center of the parallelepiped. The high and sharp peaks indicate that highly crystalline nature of thin film **1** and no other peaks can be found except SnO_2 (component of FTO glass). It confirms that complex **1** in thin film structure can be successfully synthesized by electrodeposited method.

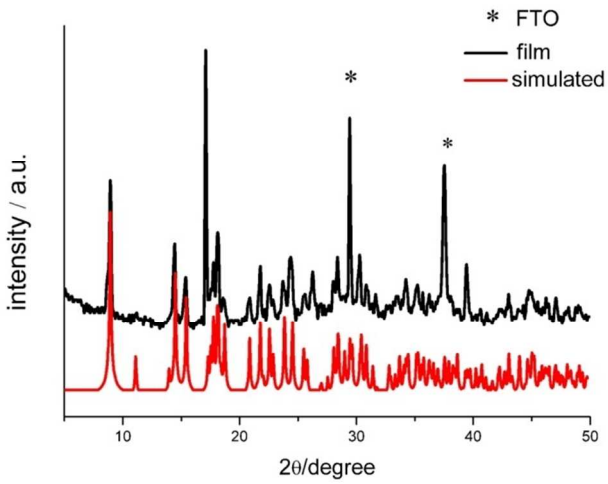

Fig. 3 Powder X-ray diffraction patterns of electrodeposited thin film **1**

3.3 Selective detection of Cu^{2+}

The solid-state luminescence spectrum of thin film **1** is investigated upon excitation at 323 nm under room temperature, which exhibits four characteristic peaks of Tb^{3+} ($^5D_4 \rightarrow {}^7F_6$: 492

nm, $^5D_4 \rightarrow {}^7F_5$: 546 nm, $^5D_4 \rightarrow {}^7F_4$: 580 nm, and $^5D_4 \rightarrow {}^7F_3$: 623 nm) (Fig. S3). It is well-known that the luminescence of Tb^{3+} has a low molar absorptivity and that the f-f transitions are spin and parity-forbidden. However, it has been shown that the lanthanide-centered emission can be sensitized by electron conjugated systems with efficient energy-transfer, which is the so-called "antenna effect". The most prominent line in film **1** is presented at 546 nm which can be observed as bright green light by naked eyes. The strong visible emission provides the possibility of film **1** as a luminescence sensor.

Selectivity is a very important parameter to evaluate the performance of the luminescence sensing system. The luminescence response of thin film **1** immerse in DMF solution containing the same concentrations of $M(NO_3)_x$ (M= Co^{2+}, Ni^{2+}, Zn^{2+}, Cd^{2+}, K^+, Na^+, Pb^{2+} and Cu^{2+}) is shown in Fig 4. Interestingly, the Cu^{2+} ion shows a significant quenching effect on the luminescence intensity of thin film **1**. However, other metal ions have slightly influence on luminescent intensity of film **1**. (Fig. 4, blue bars).

The impacts of some coexisting metal ions on Cu^{2+} ion sensing are also determined. When we add 1×10^{-3} M of Cu^{2+} to the above ions solution, it gives rise to a drastic quenching effect which is analogous to the addition of 1×10^{-3} M of Cu^{2+} alone (Fig. 4, red bars). These results indicate that these coexistent ions have negligible interfering effect on Cu^{2+} ion sensing by the film **1**.

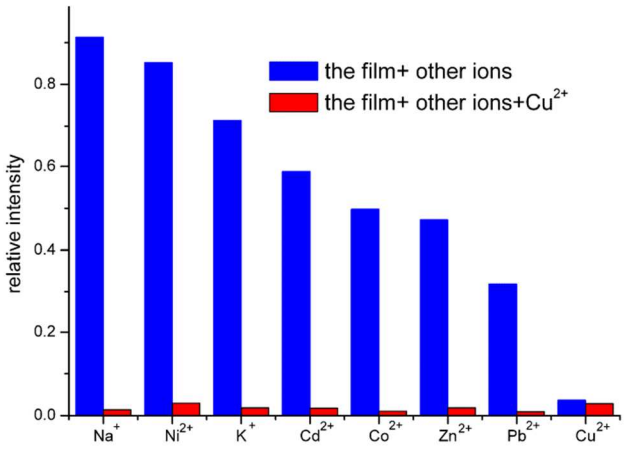

Fig. 4 Luminescence intensity at 546 nm of thin film **1** treated with different metal ions in DMF solutions. The blue bars represent the luminescence intensity of film **1** in the presence of 1×10^{-3} M of miscellaneous metal ions. The red bars represent the quenching degree of the emission that occurs upon the subsequent addition of 1×10^{-3} M of Cu^{2+} to the above solution.

Concentration-dependent luminescence measurements are examined. As shown in Fig. 5, the luminescence intensity gradually decreases with the increase of Cu^{2+} ions concentration. When the concentration of Cu^{2+} ions reaches 1×10^{-3} M, the luminescent intensity of thin film **1** becomes very weak.

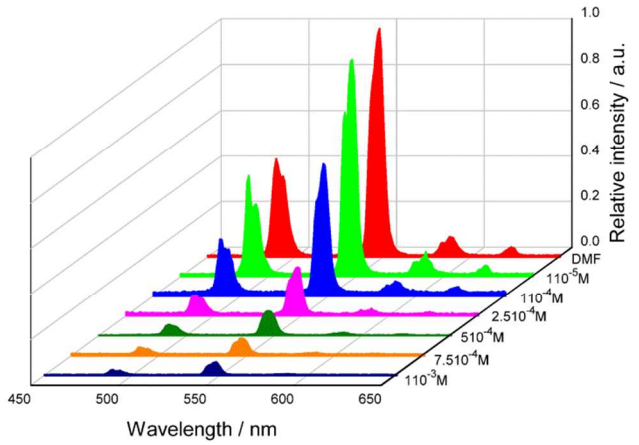

Fig. 5 Emission spectra of thin film **1** immersed in different concentrations of 1×10^{-5}-1×10^{-3} M Cu^{2+} in DMF solution when excited at 323 nm.

3.4 Possible sensing mechanism

In general, quenching mechanisms include energy transfer, excited state reactions, complex formation and collisional quenching.[40] To explain the possible mechanism of our detection system, we attempt to fit Stern-Volmer relationship to describe the concentration of Cu^{2+} ions dependence on the luminescence intensity of film **1**.

Fig.6 shows the Stern-Volmer analysis of the quenching experiment (F_0/F versus concentration of Cu^{2+}). $F_0/F = 1+K_{SV}$ [M]. It exhibits a linear relationship in the range of 1×10^{-5}-1×10^{-3} M. K_{SV} is calculated by linear regression of the plots was 1.7×10^4 / M.

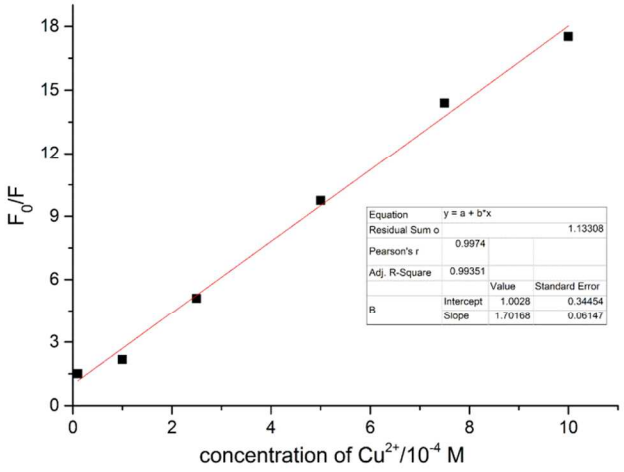

Fig. 6 Stern–Volmer plots describe the dependency of the luminescent intensities on the Cu^{2+} concentration over the range of 1×10^{-5}-1×10^{-3} M Cu^{2+} in DMF solution.

The luminescence decays of thin film **1** (before and after adding Cu^{2+} ions to the DMF solution) are investigated. The curves of luminescence decay at 546 nm are illustrated in Fig. 7. The luminescence decays of thin film 1 should be single exponential,[40] but the decay curves follow the double exponential law, and the equation $I_t = A+B_1\times\exp(-t/\tau_1)+B_2\times\exp(-t/\tau_2)$ (τ_1 and τ_2 are the fast and slow components of luminescence lifetime. *A*, B_1,

B_2 are the weighting parameters) is used for fitting the luminescence curves. The equations are stated as follows:

$$I_t = 2.086+2896.261\times\exp(-t/\tau_1)+6918.505\times\exp(-t/\tau_2)$$

$\tau_1 = 1.1$ms (82%) $\tau_2 = 0.6$ ms (18%) (Before adding Cu^{2+} ions)

$$I_t = 1.037+1070.442\times\exp(-t/\tau_1)+4454.212\times\exp(-t/\tau_2)$$

$\tau_1 = 1.0$ ms (91%) $\tau_2 = 0.4$ ms (9%) (After adding Cu^{2+} ions)

It should be attributed to DMF coordinates to Tb^{3+} ions located on the surface of crystals resulting in discrepant coordinated environments between the exterior and interior Tb^{3+} ions. The emission with the shorter luminescence lifetime should be from the exterior Tb^{3+}ions due to the vibration of the coordinated DMF molecules.[41] According to reference,[42] the average biexponential-lifetime τ can be calculated by an expression: $\tau = (B_1\tau_1^2 + B_2\tau_2^2) / (B_1\tau_1 + B_2\tau_2)$. The fitted values of the parameters A, B_1, B_2, τ_1 and τ_2 are illustrated in Table 1. According to the previous reference[38], before (τ_b) and after (τ_a) introducing Cu^{2+} ions to DMF solution, the average luminescence lifetimes remain almost the same (τ_b/τ_a=1.09). The suggestion is that the mechanism of the quenching process would be static quenching rather than dynamic quenching in this case. We speculate that Cu^{2+} may influence the photophysical properties of the ligand with a binding process, affecting the rate of energy transfer onto the Tb^{3+}, henceforth the luminescence intensity. In contrast, other ions, for instance, K^+ and Na^+ have almost no effect on the "antenna effect".

Table 1 The values of luminescence lifetime τ_1 and τ_2, the weighting parameters A, B_1, B_2, average lifetime of τ, goodness χ^2 and R^2.of fits.

Sample	A	B_1	B_2	τ_1	τ_2	τ	χ^2	R^2
Film 1	2.086	2896.261	6918.505	1.1	0.6	1.023	1.159	0.9996
Film1+ Cu^{2+}	1.037	1070.442	4454.212	1.0	0.4	0.934	1.064	0.9995

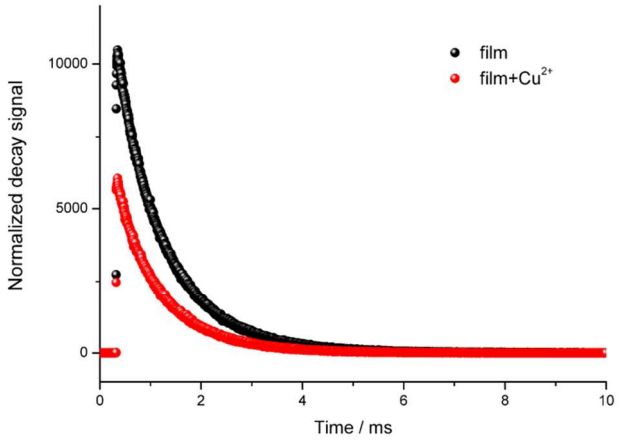

Fig. 7 Luminescence decay curves of thin film **1** in the absence and presence of Cu^{2+}.

Conclusions

A luminescent thin film **1** is successfully prepared by a facile one-step electrodeposited method in only a few minutes at room temperature. Optimized condition for the synthesis of film **1** is obtained. According to luminescent response to various metal ions, thin film **1** shows good selectivity to Cu^{2+} over other metal ions. The linear range of the luminescent relative intensity versus the Cu^{2+} concentrations is 1×10^{-5}-1×10^{-3} M. Luminescence lifetime experiment demonstrates the quenching mechanism appears to be predominantly of the static type. Future research focuses on two points of interest in our lab: effective electrodeposited method develops luminescent Ln-CPs film; and more types of Ln-CPs film for selective sensing of other interested species.

Acknowledgements

The authors acknowledge the financial support of the National Natural Science Foundation of China (51472275, 20973203 and 91022012) and the Fundamental Research Funds for the Central Universities.

Notes and references

[a] *MOE Key Laboratory of Bioinorganic and Synthetic Chemistry, KLGHEI of Environment and Energy Chemistry, School of Chemistry and Chemical Engineering Sun Yat-Sen University, Guangzhou, 510275, P.R. china. Tel: 86-20-84112977; E-mail: cesyyy@mail.sysu.edu.cn*

† Electronic Supplementary Information (ESI) available: [details of any supplementary information available should be included here]. See DOI: 10.1039/b000000x/

1. S. M. F. Vilela, A. D. G. Firmino, R. F. Mendes, J. A. Fernandes, D. Ananias, A. A. Valente, H. Ott, L. D. Carlos, J. Rocha, J. P. C. Tome and F. A. A. Paz, *Chem. Commun.*, 2013, **49**, 6400-6402.
2. Z. J. Lin, Z. Yang, T. F. Liu, Y. B. Huang and R. Cao, *Inorg.Chem.*, 2012, **51**, 1813-1820.
3. B. Chen, Y. Yang, F. Zapata, G. Lin, G. Qian and E.B. Lobkovsky. Adv. Mater., 2007, **19**, 1693-1696.
4. X.-Q. Song, L. Wang, M.-M. Zhao, G.-Q. Cheng, X.-R. Wang and Y.-Q. Peng, *Inorg. Chim. Acta*, 2013, **402**, 156-164.
5. S. Comby, E. M. Surender, O. Kotova, L. K. Truman, J. K. Molloy and T. Gunnlaugsson, *Inorg.Chem.*, 2014, **53**, 1867-1879.
6. Q. Tang, S. X. Liu, Y. W. Liu, J. Miao, S. J. Li, L. Zhang, Z. Shi and Z. P. Zheng, *Inorg.Chem.*, 2013, **52**, 2799-2801.
7. Cai, D. N., Guo, H. L., Wen, L., Liu, C. G, *Crystengcomm.*, 2013, 34, 2702-2708
8. K. L. Wong, G. L. Law, Y. Y. Yang and W. T. Wong, *Adv. Mater.*, 2006, **18**, 1051-1054.
9. S. Nadella, P. M. Selvakumar, E. Suresh, P. S. Subramanian, M. Albrecht, M. Giese and R. Frohlich, *Chem-Eur. J.*, 2012, **18**, 16784-16792.
10. R. Ameloot, L. Pandey, M. Van der Auweraer, L. Alaerts, B. F. Sels and D. E. De Vos, *Chem.Commun.*, 2010, **46**, 3735-3737.
11. H. L. Guo, Y. Z. Zhu, S. L. Qiu, J. A. Lercher and H. J. Zhang, *Adv. Mater.*, 2010, **22**, 4190-4192.
12. O. Shekhah, J. Liu, R. A. Fischer and C. Woll, *Chem. Soc. Rev.*, 2011, **40**, 1081-1106.
13. A. Domenech, H. Garcia, M. T. Domenech-Carbo and F. Xamena, *Electrochem. Commun.*, 2006, **8**, 1830-1834.
14. Z. S. Dou, J. C. Yu, H. Xu, Y. J. Cui, Y. Yang and G. D. Qian, *Micropor. Mesopor. Mater.*, 2013, **179**, 198-204.
15. Z. S. Dou, J. C. Yu, Y. J. Cui, Y. Yang, Z. Y. Wang, D. R. Yang and G. D. Qian, *J. Am.Chem. Soc.*, 2014, **136**, 5527-5530.

16. Nicolò Campagnol, Ernesto Rezende Souza, Dirk E. De Vos, Koen Binnemans and Jan Fransaer, *Chem. Commun.*, 2014, **50**, 12545-12547.
17. Eliseeva, S. V., Pleshkov, D. N., Lyssenko, K. A., Lepnev, L. S.,Bunzli, J. C. G., Kuzminat, N. P., *Inorg. Chem*., 2010, **49**, 9300-9311.
18. L. W. Han, J. A. Lu, T. F. Liu, S. Y. Gao and R. Cao, *Dalton Trans.,* 2010, **39**, 10967-10973.
19. I. Gurrappa and L. Binder, *Sci. Tech . Adv. Mater*., 2008, **4**, 1-11.
20. C. Boeckler, A. Feldhoff and T. Oekermann, *Adv. Funct. Mater.*, 2007, **17**, 3864-3869.
21. M. Y. Li and M. Dinca, *Chem. Sci.*, 2014, **5**, 107-111.
22. A. Domenech, H. Garcia, M. T. Domenech-Carbo and F. Xamena, *J. Phy. Chem.*, 2007, **111**, 13701-13711.
23. B. Van de Voorde, R. Ameloot, I. Stassen, M. Everaert, D. De Vos and J. C. Tan, *J. Mater. Chem. C*, 2013, **1**, 7716-7724.
24. M. Y. Li and M. Dinca, *J. Am. Chem. Soc.*, 2011, **133**, 12926-12929.
25. K. Y. Cheng, J. C. Wang, C. Y. Lin, W. R. Lin, Y. A. Chen, F. J. Tsai, Y. C. Chuang, G. Y. Lin, C. W. Ni, Y. T. Zeng and M. L. Ho, *Dalton Trans.*, 2014, **43**, 6536-6547.
26. R. S. Kumar, S. S. Kumar and M. A. Kulandainathan, *Micropor. Mesopor. Mater.*, 2013, **168**, 57-64.
27. F. X. Wang, Z. Y. Gu, W. Lei, W. J. Wang, X. F. Xia and Q. L. Hao, *Sensors & Actuat. B-Chem.*, 2014, **190**, 516-522.
28. R. J. Xie, Y. R. Yi, Y. He, X. G. Liu and Z. X. Liu, *Tetrahedron*, 2013, **69**, 8541-8546.
29. P. Singh, R. Kumar and S. Kumar, *J. Fluoresc.*, 2014, **24**, 417-424.
30. M. H. Mashhadizadeh, M. Pesteh, M. Talakesh, I. Sheikhshoaie, M. Mazloum-Ardakani and M. A. Karimi, *Spectrochim. Acta B*, 2008, **63**, 885-888.
31. S. L. C. Ferreira, A. S. Queiroz and M. S. Fernandes, *Acta Part B: Atomic*, 2002, **57**,1939-1950.
32. M. Arvand and Z. Lashkari, *Spectrochim. Acta A*, 2013, **107**, 280-288.
33. Y.-M. Zhu, C. H. Zeng, T. S. Chu, H. M. Wang, Y. Y. Yang, Y. X. Tong, C. Y. Su and W. T. Wong, *J. Mater. Chem. A*, 2013, **1**, 11312-11319.
34. C. H. Zeng, F. L. Zhao, Y.-Y. Yang, M. Y. Xie, X. M. Ding, D. J. Hou and S. W. Ng, *Dalton Trans.*, 2013, **42**, 2052-2061.
35. C.-H. Zeng, J.-L. Wang, Y.-Y. Yang, T.-S. Chu, S.-L. Zhong, S. W. Ng and W. T. Wong, *J. Mater. Chem. C*, 2014, **2**, 2235-2242.
36. H.-M. Wang, Y. Y. Yang, C.-H. Zeng, T. S. Chu, Y. M. Zhu and S. W. Ng, *Photoch. Photobio. Sci.*, 2013, **12**, 1700-1706.
37. X. D. Guo, G. S. Zhu, F. X. Sun, Z. Y. Li, X. J. Zhao, X. T. Li, H. C. Wang and S. L. Qiu, *Inorg. Chem.*, 2006, **45**, 2581-2587.
38. L. J. Fan, Y. Zhang, C. B. Murphy, S. E. Angell, M. F. L. Parker, B. R. Flynn and W. E. Jones, Jr., *Coord. Chem. Rev.*, 2009, **253**, 410-422.
39. A. Martinez Joaristi, J. Juan-Alcañiz, P. Serra-Crespo, F. Kapt eijn and J. Gascon, *Cryst. Growth Des.*, 2012, **12**, 3489-3498.
40. T. M. Reineke, M. Eddaoudi, M. Fehr, D. Kelley and O. M. Yaghi, *J. Am. chem. Soc.*, 1999, **121**, 1651-1657.
41. X. H. Zhou, L. Li, H. H. Li, A. Li, T. Yang and W. Huang , *Dalton Trans.*, 2013, **42**, 12403-12409.
42. Y. L. Ding, Shirly. Z. Shen, H.D. Sun, H. N. Sun, F. T. Liu, *Sensors & Actuat. B-Chem.*, 2014, **203**, 35-43.

